Structural and magnetic properties of $(Fe_{0.93}Ni_{0.07})_2P$

2007 J. Phys.: Condens. Matter 19 196217

(http://iopscience.iop.org/0953-8984/19/19/196217)

IOP PUBLISHING JOURNAL OF PHYSICS: CONDENSED MATTER

J. Phys.: Condens. Matter **19** (2007) 196217 (12pp) doi:10.1088/0953-8984/19/19/196217

Structural and magnetic properties of $(Fe_{0.93}Ni_{0.07})_2P$

Sudhish Kumar[1,4], **Anjali Krishnamurthy**[2], **Bipin K Srivastava**[2] and **S K Paranjpe**[3,5]

[1] Department of Physics, M L Sukhadia University, Udaipur 313 002, India
[2] Department of Physics, University of Rajasthan, Jaipur 302 004, India
[3] Solid State Physics Division, Bhabha Atomic Research Centre, Mumbai 400 085, India

E-mail: skmlsu@gmail.com

Received 23 January 2007, in final form 2 March 2007
Published 19 April 2007
Online at stacks.iop.org/JPhysCM/19/196217

Abstract

Structural and magnetic properties of $(Fe_{0.93}Ni_{0.07})_2P$ have been investigated by means of powder x-ray and neutron diffraction, magnetization and paramagnetic susceptibility measurements over a temperature range of 10–500 K. The system crystallizes in the Fe_2P type hexagonal structure ($P\bar{6}2m$ space group, $Z = 3$) in which the Ni atoms occupy the tetrahedral M_I sites with total preference. Refined values of the cell parameters and bond distances are found slightly higher than those for Fe_2P and the atomic positional parameters are found quite close to those reported for the parent compound Fe_2P. The temperature dependence of the magnetization shows a sharp magnetic phase transition around 298(5) K. However there is difference of the zero-field cooled and field cooled modes of the magnetization, which is indicative of the formation of ferromagnetic clusters. The ferromagnetic to paramagnetic transition shifts towards the higher temperature side with increase in the applied magnetic field, which indicates that the phase transition is a field induced type first-order magnetic phase transition. There is no crystallographic structural transition associated with the magnetic phase transition. The transition is caused by the change in the c/a ratio. The alloy retains the ferromagnetic order of Fe_2P with the moments orienting along the [001] direction. The Rhodes–Wohlfarth ratio (μ_p/μ_s) of $(Fe_{0.93}Ni_{0.07})_2P$ is found to be 1.53 (>1), showing itinerant magnetism in this compound. At 297 K the magnetic moment at the M_I site is found negligible but at the M_{II} site it is $\sim$0.51 μ_B. The observed non-linearity above T_c in the χ^{-1}–T curve gives clear evidence of the presence of short range magnetic order above T_c. The moments at the M_{II} sites in the paramagnetic state and the exchange interactions are responsible for the short range one-dimensional ferromagnetic chains along [001] well above the T_c in $(Fe_{0.93}Ni_{0.07})_2P$.

[4] Author to whom any correspondence should be addressed.
[5] Present address: NAPC, International Atomic Energy Agency, Vienna, Austria.

0953-8984/07/196217+12$30.00

1. Introduction

Transition metal pnictides with general formula $(Fe_{1-x}M_x)_2P$ (where M = Cr, Mn, Co and Ni) have been the subject of intensive investigation owing to their interesting magnetic behaviours/structures, magnetoelastic phase transitions and magnetocaloric effects [1–8]. In these compounds there is a subtle balance of ferromagnetic and antiferromagnetic exchange interactions. Low level substitution of Ni for Fe in Fe_2P strengthens the ferromagnetic ordering. All the compounds in the series $(Fe_{1-x}Ni_x)_2P$, up to $x = 0.50$ are ferromagnetic and Ni_2P is paramagnetic. Initially in the low level Ni substituted alloys T_c increases sharply [2–4]. As against a value of 216 K for Fe_2P, the values of T_c for $x = 0.01$ and 0.05 are ∼235 and ∼295 K [4]; for $x = 0.10$, T_c is maximum at ∼342 K [3]. Magnetocrystalline anisotropy decreases with introduction of Ni for Fe [3]. Mössbauer results showed that for low level Ni substitution, Ni atoms preferentially occupy the tetrahedral sites and the hyperfine fields reduce at both the crystalline sites [5]. In our previously reported neutron diffraction study on $(Fe_{0.93}Ni_{0.07})_2P$, we have shown that the values of magnetic moments at the two metallic sites do not change much and the moments continue to orient along the *c*-axis as in the parent compound Fe_2P [6, 7].

Zach *et al* investigated the magnetoelastic properties and electronic structures of the $(Fe_{1-x}Ni_x)_2P$ system [8]. They have shown that low level Ni substituted compounds show a first-order ferromagnetic to paramagnetic phase transition. Strong electron polarization at E_F is responsible for the magnetoelastic phase transitions in the compounds with small substitution of Ni for Fe in Fe_2P [8]. The magnetic properties of these compounds are quite similar to those of the magnetocaloric materials like $MnFeP_{1-y}As_y$ [9, 10].

In our recent neutron diffraction study on the magnetic structure of $(Fe_{0.70}Co_{0.30})_2P$, we have shown that Co atoms occupy the tetrahedral sites with ∼95% preference. The compound, unlike Fe_2P, is a non-collinear ferromagnet with moments orienting at $\vartheta = 45°$ and $\phi = 30°$ for the tetrahedral M_I sites and $\vartheta = 15°$ and $\phi = 5°$ for the pyramidal M_{II} sites [11]. In another recent study, Sun *et al* reported metal–insulator transition and magnetoresistance effects in $Co_xFe_{1-x}MnP$ compounds [12]. Thus due to their peculiar magnetic properties these transition metal pnictides have continued to attract attention.

In the present work we have undertaken detailed magnetization, paramagnetic susceptibility and powder x-ray and neutron diffraction measurements on the structural and magnetic properties of $(Fe_{0.93}Ni_{0.07})_2P$.

2. Experimental details

The alloy $(Fe_{0.93}Ni_{0.07})_2P$ (hereafter referred to as FNP7) was prepared by the technique of solid state diffusion at ∼1000 °C as described in [6]. High purity Fe powder (4N), Ni powder (4N), and red P flakes (5N) were used as the starting materials. In order to ensure the homogeneity and single-phase nature of the samples, x-ray diffraction (XRD) patterns were recorded after each heat treatment.

Powder x-ray diffraction measurements using Mn filtered monochromatic Fe Kα radiation ($\lambda = 1.937\,355$ Å) were made in the 2θ range of 3°–100° using a Philips x-ray powder diffractometer (PW1840). A silicon sample (cubic with $a = 5.431$ Å in a plate form) was used as a standard sample for internal calibration for angle 2θ.

Temperature and field dependent magnetization measurements on the sample were performed in the temperature range 85–500 K and in fields up to 8.0 kOe using the Princeton Applied Research Co. make vibrating sample magnetometer (model 155). For low temperature measurements the sample was packed in a Perspex cup and then placed in a flow control type

Janis make liquid nitrogen cryostat. For the high temperature measurements in the range of 300 K $< T <$ 500 K the sample was packed in a silver cup and then placed in a high temperature oven (PARC make, model 155). The samples were demagnetized before each magnetization versus temperature and magnetization versus magnetic field measurement.

Temperature dependent neutron diffraction (ND) measurements were made on the sample in powder form at the 100 MW 'Dhruva' Reactor at the Bhabha Atomic Research Centre, Mumbai. Diffraction patterns were recorded on a position sensitive detector based powder diffractometer [13, 14]. A neutron beam of wavelength $\lambda = 1.094$ Å was used. For low temperature measurements down to 10 K, a closed helium cycle refrigerator (CCR) cryostat was used. For room temperature (297 K) measurement, ∼10 g powder sample was packed in a cylindrical vanadium container which was then loaded on the diffractometer in air. The room temperature pattern was recorded in the 2θ range of 10°–80°.

For low temperature measurements, the powdered sample was packed in an aluminium sample holder (for ensuring good thermal conductivity and less incoherent scattering). The only problem with aluminium is that its diffraction peaks may interfere with those of the sample. This aspect has been taken care of during profile refinement of the diffraction patterns. The sample holder was attached to the cold finger of an evacuated closed helium cycle refrigerator cryostat.

ND patterns were recorded at 10, 40, 80, 120, 250 and 297 K. Rietveld profile refinements of the ND patterns were carried out using the FULLPROF Program [15], where the magnetic part of the diffraction pattern can be treated as an additional 'phase'. In the nuclear structure refinement the parameters varied were: two cell parameters, two atomic positions, site occupancies, overall isotropic temperature factor in addition to the instrumental parameters such as zero angle, three halfwidth parameters and a scale factor. From the observed pattern the background points corresponding to different angles have been directly fed in as input. The profile shape has been taken as a Gaussian function and a peak asymmetry correction was made for 2θ below 25°. The nuclear scattering lengths used in the analysis are: $b_{\mathrm{Fe}} = 9.45$ fm, $b_{\mathrm{Ni}} = 10.3$ fm and $b_{\mathrm{P}} = 5.13$ fm.

For determination of the magnetic structure, low temperature diffractograms (i.e., in the magnetic state) have been analysed using the magnetic profile refinement method, in which the magnetic phase was treated as a second phase in addition to the nuclear phase. In the magnetic refinement, site occupancies obtained from the analysis of the 297 K pattern were kept constant and in addition the magnetization for the two metallic sites has been refined. The form factors corresponding to different ions have been taken from the paper of Watson and Freeman [16] and directly fed into the refinement program.

3. Results and discussion

In the XRD pattern of FNP7 all the reflections were indexed in Fe_2P type hexagonal symmetry and no detectable peak from any other phase was observed. This confirms that the alloy has been formed in single phase. The cell parameters were finally refined with the help of a least squares refinement program. The cell parameters obtained for FNP7 are $a = 5.892(2)$ Å and $c = 3.471(2)$ Å. These values are slightly higher than those reported for Fe_2P [17].

Rietveld refinement of the 297 K ND pattern was carried out using the $P\bar{6}2m$ space group ($Z = 3$), with the two metal atoms at the tetrahedral M_I sites (surrounded by four phosphorus atoms in a tetrahedral arrangement) in 3f and at the pyramidal M_{II} sites (surrounded by five phosphorus atoms in a pyramidal arrangement) in 3g. The phosphorus atoms are at the P_I sites in 2c positions and P_{II} sites in 1b positions. The temperature 297 K falls in a region of ferromagnetic to paramagnetic transition and the sample is not completely paramagnetic at

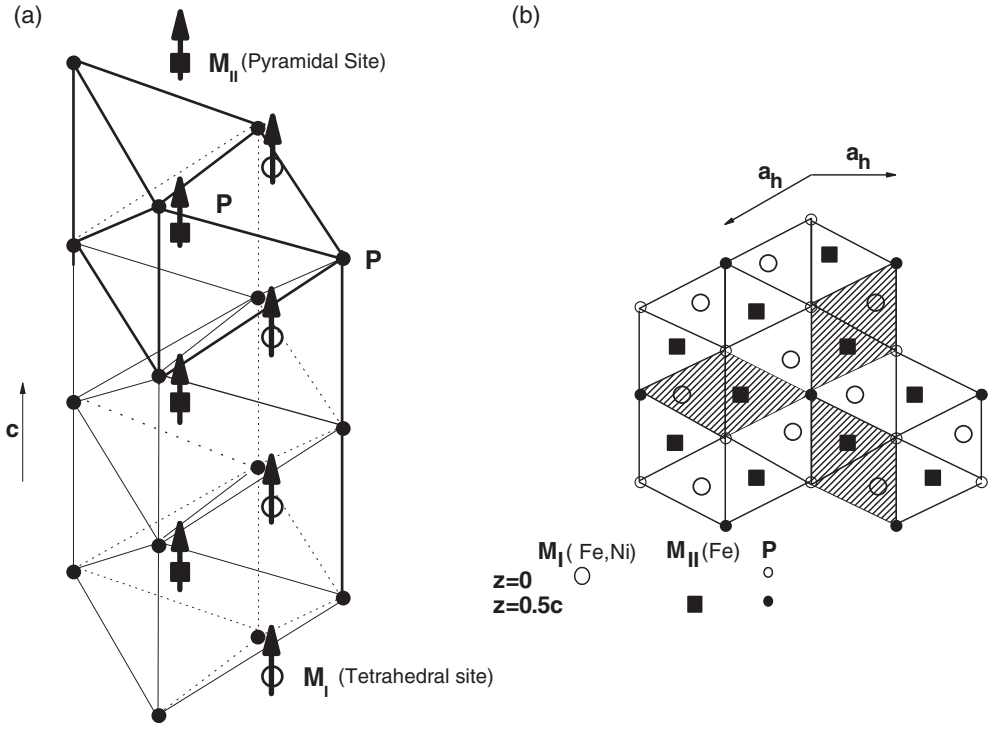

Figure 1. (a) Basic building block of the hexagonal form—a rhombohedral cell $M_IM_{II}P$ containing tetrahedrally coordinated M_I and pyramidally coordinated M_{II} metal atoms (also showing the magnetic structure of $(Fe_{0.93}Ni_{0.07})_2P$) and (b) the hexagonal Fe_2P structure projected onto the *ab* plane.

this temperature. Therefore the refinement was done both for the nuclear as well as for the magnetic phase. First the nuclear structure of FNP7 was refined using the diffraction pattern in the higher angle region where magnetic scattering makes a negligible contribution; after fixing all the parameters the magnetic phase was included in the analysis and refined. The site occupancies at the two metallic positions (M_I in 3f and M_{II} in 3g) and the two P positions (P_I in 2c and P_{II} in 1b) were constrained in order to keep the sum of metal ions and P ions at the two sites always having its stoichiometric value. The crystal structure is illustrated in figure 1, in which we depict (a) the basic building block of the hexagonal structure which is a rhombohedral cell $M_IM_{II}P$, (b) the hexagonal Fe_2P structure projected onto the *ab* plane.

Figure 2 shows the fitted ND pattern at 297 K. The results are listed in table 1. The analysis shows that Ni atoms occupy the tetrahedral (M_I) sites with total preference. Thus the M_{II} sites are fully occupied by Fe atoms; while both Fe and Ni atoms are randomly distributed at the M_I sites. The obtained values of cell parameters are found slightly higher than those for Fe_2P and the atomic positional parameters are found quite close to those reported for the parent compound Fe_2P. The inter-atomic distances in the alloy at 297 K, computed using the atomic position coordinates in the space group $P\bar{6}2m$ and the lattice constants, are listed in table 2. Also listed are the distances reported for Fe_2P [17]. It is noted that the distances in the composition under study are quite close to those in Fe_2P. This is in conformity with the fact that the alloy under study crystallizes in the Fe_2P type hexagonal structure. Further $d(M_I–P)$ are smaller than $d(M_{II}–P)$. Thus the electron transfer from P atoms to M_I atoms is larger than

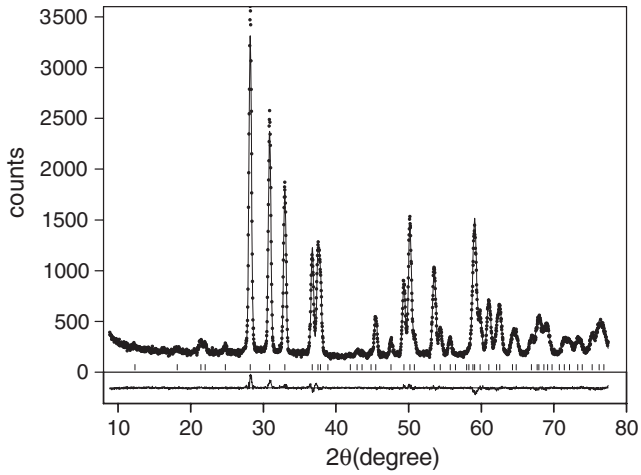

Figure 2. Neutron diffraction patterns of $(Fe_{0.93}Ni_{0.07})_2P$ at 297 K. Observed (calculated) profiles are shown by dotted (solid) lines. The short vertical marks represent Bragg reflections. The lower curve is the difference plot.

Table 1. Crystallographic data for $(Fe_{0.93}Ni_{0.07})_2P$ obtained using the Rietveld refinement of the powder neutron diffraction pattern at 297 K. (Note: The numbers in the parentheses are estimated standard deviations referred to the last significant digit.)

Space group: $P\bar{6}2m$ (No. 189, $Z = 3$)
Cell parameters: $a = 5.882(3)$ Å, $c = 3.473(4)$ Å
Unit cell volume $= 104.37(1)$ Å^3
Overall isotropic temperature factor (B_o) $= 0.3568($ Å$^2)$
Halfwidth parameters: $U = 2.436\,615$, $V = -1.5063$ and $W = 0.40$
Agreement factors (R-factors): $R_p = 4.75$, $R_{wp} = 6.16$, $R_{expected} = 5.10$, $R_{nuclear} = 1.81$, $R_{magnetic} = 2.31$ and $R_{Bragg} = 3.23$
Goodness of fit (S) $= 1.20$

Positional parameters, site occupations and magnetic moments pointing along the [001] direction at the two metallic sites M_I and M_{II}.

Site	Position	x	y	z	Occupancy	Moment (μ_B)
M_I	3f	0.2570(2)	0	0	0.86Fe + 0.14Ni	0.08(4)
M_{II}	3g	0.5949(2)	0	0.5	1.0Fe	0.51(2)
P_I	2c	1/3	2/3	0	0.667P	—
P_{II}	1b	0	0	0.5	0.333P	—

to M_{II} atoms implying a greater mixing of p bands of P atoms with d bands of M_I atoms than with d bands of M_{II} atoms. These facts and that Ni has more valence electrons than Fe would explain the observed total preference of Ni atoms for M_I sites [1].

Figures 3(a) and (b) show the temperature (T) dependence of the magnetization (M) recorded in the zero-field cooled (ZFC) and field cooled (FC) modes in the region 85–315 K under external magnetic fields of 50 Oe and 175 Oe respectively. These two M versus T curves show a Brillouin function type of variation, which is suggestive of ferromagnetic (FM) nature of the compound. In the ferromagnetic region instead of flattening, the magnetization shows an upward trend. There is a large difference of the ZFC and FC modes, which is indicative of the formation of magnetic clusters in the systems. It is also to be noted that the FC curve lies well

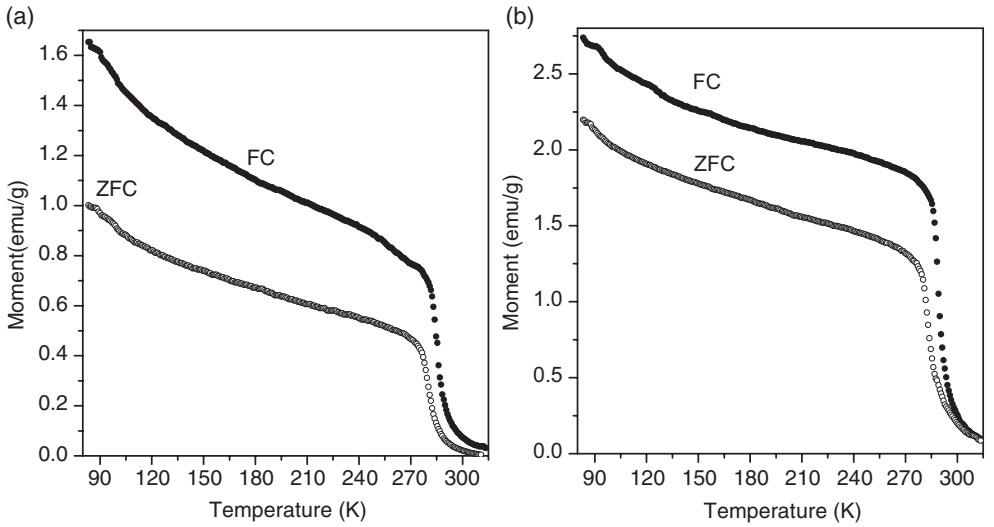

Figure 3. Magnetic moment, recorded in zero-field cooled (ZFC) and field cooled (FC) modes as a function of temperature under an external magnetic field of (a) 50 Oe and (b) 175 Oe.

Table 2. Inter-atomic distances (Å) in the alloy $(Fe_{0.93}Ni_{0.07})_2P$ at 297 K. Also for comparison are given the distances, as reported in literature [17] for Fe_2P. Distances shorter than 3.10 Å are listed. M_I = (Fe, Ni) and M_{II} = Fe.

Bonds	$(Fe_{0.93}Ni_{0.07})_2P$	Fe_2P	Bonds	$(Fe_{0.93}Ni_{0.07})_2P$	Fe_2P
M_I–$2P_I$	2.221	2.215	M_{II}–$1P_{II}$	2.384	2.379
M_I–$2P_{II}$	2.304	2.294	M_{II}–$4P_I$	2.494	2.483
M_I–$2M_I$	2.622	2.610	M_{II}–$2M_I$	2.641	2.630
M_I–$2M_{II}$	2.641	2.630	M_{II}–$4M_I$	2.717	2.708
M_I–$4M_{II}$	2.717	2.708	M_{II}–$4M_{II}$	3.099	3.087

above the ZFC one even above T_c. This is suggestive of short range magnetic order persisting to quite high temperatures well above the Curie point [1]. The corresponding dM/dT as a function of temperature curves are shown in the figures 4(a) and (b). It is interesting to note that the ZFC and FC modes are peaking at different temperatures and the peaks shift towards the higher temperature side with increase in the field. In order to understand these features more clearly we have recorded the magnetization as a function of temperature in a high magnetic field. Figure 5 shows the M versus T curve recorded in the FC mode in an external field of 1000 Oe. The Brillouin curve appearance of this M–T curve shows a sharp transition from a ferromagnetic to a paramagnetic state. The abrupt change of magnetization at the transition indicates that the magnetic phase transition is of the first-order type [1, 18]. The peak in the dM/dT–T curve (depicted in figure 6) gives a Curie temperature (T_c) of 298(5) K.

Figure 7 shows the variation of the magnetization as a function of the external magnetic field (H) at 85 and 300 K. Initially, the magnetization increases rapidly with H but after ∼2 kOe the increase becomes quite sluggish. This is suggestive of a high magnetocrystalline anisotropy as in Fe_2P. Further, at 85 K and in an external magnetic field of 8 kOe, the value of the moment is ∼63 emu g^{-1} as against ∼48 emu g^{-1} for powdered Fe_2P in a field of the same strength and at a lower temperature of 10 K. The saturation magnetization M_s = 95 emu g^{-1} (2.43 μ_B/formula unit) was estimated from the M–$1/H$ curve by extrapolating

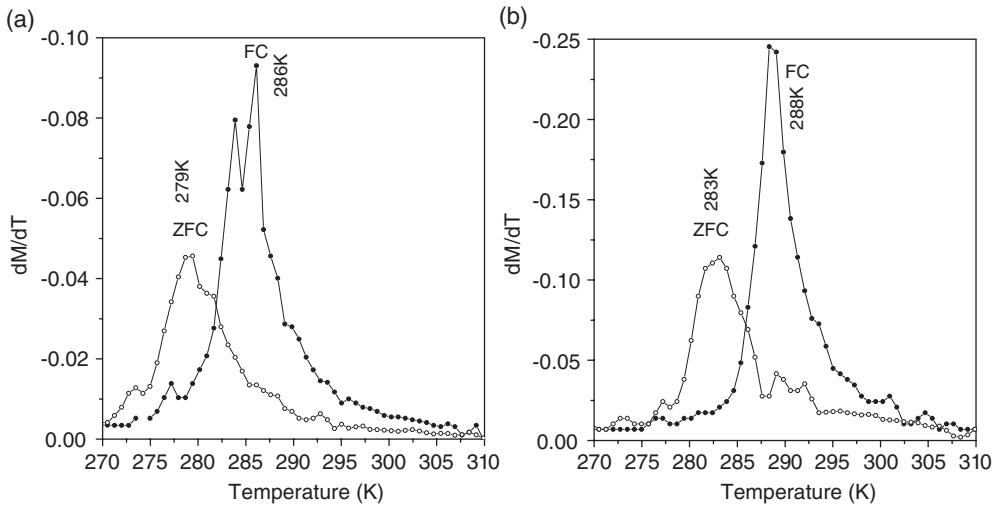

Figure 4. $\mathrm{d}M/\mathrm{d}T$ as a function of temperature under external magnetic fields of (a) 50 Oe and (b) 175 Oe.

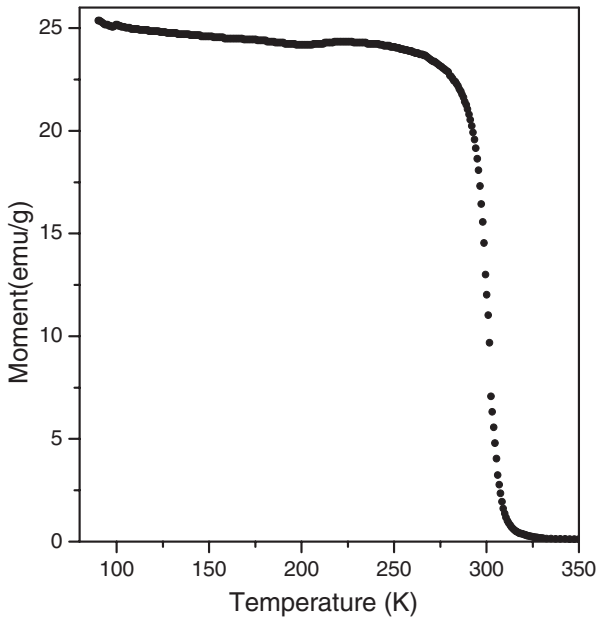

Figure 5. Magnetic moment recorded in the field cooled mode as a function of temperature under an external magnetic field of 1000 Oe.

$1/H$ to zero. The saturation moment reported for single-crystal Fe_2P is $\sim$120 emu g^{-1} [19]. However, the values of the remanence and coercive fields are rather small. These results are in good agreement with the earlier contention [2–4] that substitution of Ni (i) strengthens the ferromagnetic ordering raising the transition temperature and (ii) lowers the magnetocrystalline anisotropy.

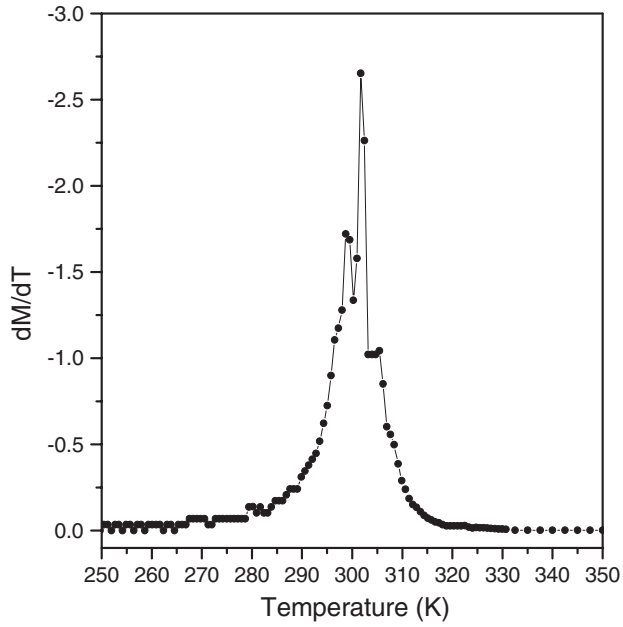

Figure 6. $\mathrm{d}M/\mathrm{d}T$ as a function of temperature under an external magnetic field of 1000 Oe.

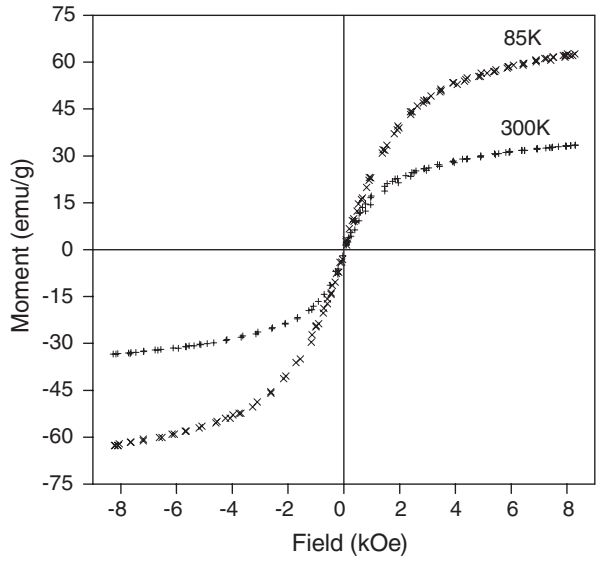

Figure 7. Magnetic moment recorded as a function of external magnetic field at 85 and 300 K.

The inverse of the paramagnetic susceptibility (χ^{-1}) versus T curve in the temperature range 300–500 K is shown in figure 8. This susceptibility curve deviates from the Curie–Weiss behaviour and the estimated paramagnetic Curie temperature (θ_p) is about 398 K, which is almost the same as that for the parent compound Fe_2P. The non-linear nature of this curve and higher (by about 100 K) value of θ_p than of T_c clearly indicates that, like in Fe_2P, short range magnetic order persists well above T_c in FNP7 [20] as also inferred above. The effective

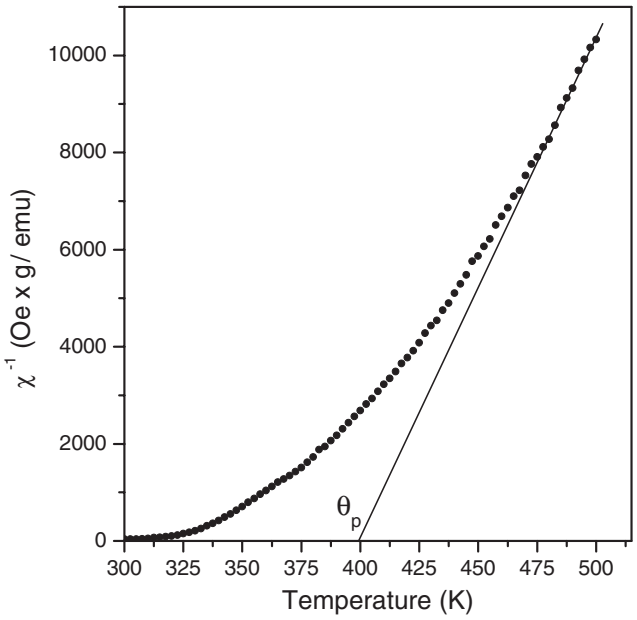

Figure 8. Inverse susceptibility (χ^{-1}) plotted as a function of temperature under an external magnetic field of 1000 Oe.

Table 3. Temperature dependence of the cell parameters and c/a ratio.

Temperature (K)	a (Å)	c (Å)	c/a
305	5.892(2)	3.471(3)	0.589
297	5.882(3)	3.473(4)	0.590
250	5.896(3)	3.464(3)	0.587
120	5.894(2)	3.456(3)	0.586
80	5.894(3)	3.456(4)	0.586
40	5.893(4)	3.455(2)	0.586
10	5.898(3)	3.457(3)	0.586

paramagnetic Bohr magneton number (P_{eff}) per formula unit, estimated (per formula unit) using χ^{-1}–T curves, is obtained to be $P_{\text{eff}} = 3.56$ and the paramagnetic magnetic moment (μ_{p}) per metal atom (there are two metals per formula unit in this case) in the paramagnetic state is estimated to be $\mu_{\text{p}} = 2.07\ \mu_{\text{B}}$/atom).

Neutron diffraction (ND) patterns recorded at different temperatures down to 10 K clearly indicate that as the temperature is lowered from 297 K, substantial enhancement occurs in the intensities of the reflections (100), (110), (101) and (200), while the intensity of the reflection (001) remains unchanged. No measurable superlattice diffraction peaks were observed in any of these patterns recorded down to 10 K ruling out the possibility of an antiferromagnetic or non-collinear ordering. These facts are suggestive of ferromagnetic ordering.

Figures 9(a) and (b) display the temperature dependence of the integrated intensity of the (110) and (200) magnetic reflections. The integrated intensities were obtained by least squares fitting of a Gaussian function. The background contribution was estimated by fitting a second-order polynomial. We notice that the nature of these curves is quite similar to that of the magnetization versus temperature curve further confirming the ferromagnetic to paramagnetic transition.

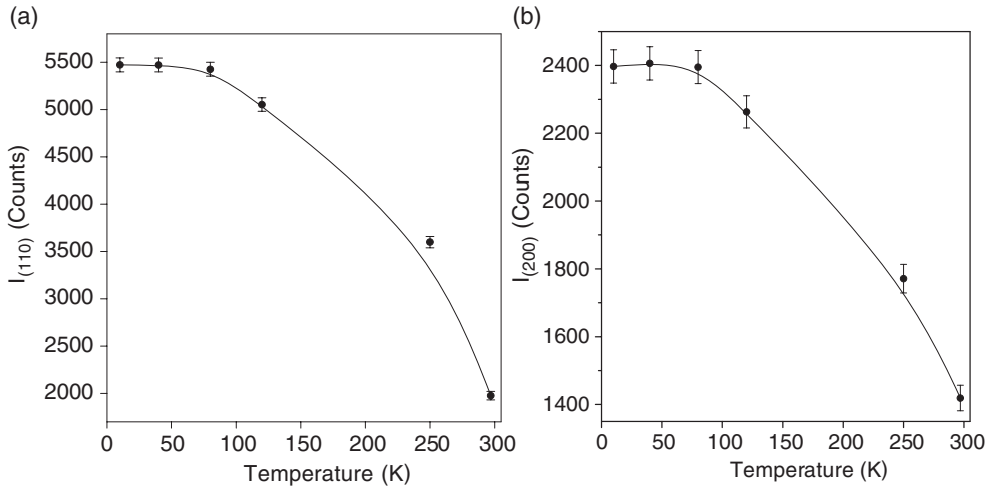

Figure 9. Temperature dependence of the integrated intensity of the magnetic reflections (a) I_{110} of (110) and (b) I_{200} of (200). The bars indicate standard deviations. The solid lines are plotted as a guide for the eye.

For obtaining the magnetic structure of FNP7, the ND patterns at different temperatures were analysed in the 2θ region of 10°–40° using the profile refinement for both the nuclear and magnetic scattering contributions. Initially the data refinement was done by assuming that the moments point along the [001] direction as in the parent compound Fe_2P. Several other attempts assuming the moments to point along other directions were also made but the best fittings were obtained when moments were assumed to be aligned along [001]. So this analysis confirms that the moments at the two sites point along [001]. The form factors corresponding to Fe^{4+} for Fe at an M_{II} site and the weighted values of Fe° and Ni° for the M_I sites were used. This is in accordance with the procedure followed by Fujii *et al* [21] in their analysis of polarized neutron diffraction data on a single crystal of Fe_2P. We have also tried analysing the patterns using the form factors corresponding to other ions of Fe but such attempts gave poor results.

The refined values of the magnetic moments at 10 K are $0.89(3)\mu_B$ at the M_I sites and $1.81(9)\mu_B$ at the M_{II} sites. At 80 K the moments are $0.80(4)\mu_B$ at the M_I sites and $1.68(8)\mu_B$ at the M_{II} sites giving $\mu_s = 2.48\mu_B$ per formula unit, which is in very good agreement with the $\mu_s = 2.43\ \mu_B$ obtained from the M–H curve at 85 K. On the other hand at 297 K the moments at the M_I sites are negligible ($0.08(4)\ \mu_B$) while that at M_{II} sites they are $0.51(2)\ \mu_B$. It is noted that the moment at an M_{II} site is almost double that at an M_I site and is slightly higher than that reported, based on a polarized ND study, in Fe_2P [21]. But it is less than what was reported on the basis of powder ND study of Fe_2P [22] and also less than what was predicted, on the basis of electronic structure calculations, for Fe_2P [1]. The magnetic structure of the alloy is shown in figure 1(a), where the vertical arrow shows the orientations of the moments at M_I and M_{II} sites to be along the [001] direction.

The variations in cell parameters and c/a ratio as a function of temperature are presented in table 3. The ratio c/a shows a big change around the transition temperature of 297 K. The transition is accompanied by discontinuous change in the dimensions of the hexagonal unit cell with decrease in a-axis length and an increase of the c-axis length. This observation further confirms the first-order nature of the magnetic transition in this alloy [1, 18].

According to the Rhodes–Wohlfarth theory the ratio μ_p/μ_s is expected to be 1 for local moment ferromagnets and larger than 1 for itinerant ferromagnets [23, 24]. It is interesting to note that in FNP7 the saturation magnetic moment per metal ion at 10 K is $\mu_s = 1.35\mu_B$ and the paramagnetic moment is $\mu_p = 2.07\ \mu_B$. Therefore this ratio $\mu_p/\mu_s = 1.53 > 1$, confirms the itinerant magnetism in this alloy. This feature was also reported for Fe_2P and for Mn substituted Fe_2P based alloys [1]. At 297 K the negligible moment at the M_I site and large magnetic moment at the M_{II} site (0.51 μ_B) clearly indicate that the momenta at the M_{II} sites in the paramagnetic state and the exchange interactions are responsible for the short range magnetic correlations (one-dimensional FM chains along [001]) far above T_c in FNP7.

4. Conclusions

$(Fe_{0.93}Ni_{0.07})_2P$ crystallizes in the Fe_2P type hexagonal structure with slightly larger lattice constants and bond distances than in Fe_2P and the positional parameters are quite close to those for Fe_2P. Magnetization measurements and the magnetic structure refinement of the powder neutron diffraction data establish its ferromagnetic nature and are suggestive of a first-order ferromagnetic to paramagnetic phase transition in $(Fe_{0.93}Ni_{0.07})_2P$.

Introduction of Ni for Fe in Fe_2P leads to strengthening of the ferromagnetic ordering in the sense of raising of T_c but the values of the moments do not change much. The moment at an M_{II} site (1.81 μ_B) at 10 K is almost double that at an M_I site (0.89 μ_B). At 297 K the moment at an M_I site is very small but at an M_{II} site it is 0.51 μ_B. Results on the field dependence of the magnetization suggest that the magnetic anisotropy has reduced as compared to that for Fe_2P but the moments at the two metallic sites continue to orient along [001] as in the parent compound Fe_2P. The observed Rhodes–Wohlfarth ratio $\mu_p/\mu_s = 1.53 > 1$ confirms an itinerant type of magnetism in these alloys. The χ^{-1} versus T curve deviates from the Curie–Weiss behaviour and the non-linearity of this curve is indicative of short range ordering above T_c. The moments at the M_{II} sites in the paramagnetic state and the exchange interactions are responsible for the short range correlations (one-dimensional FM chains along [001]) far above T_c in $(Fe_{0.93}Ni_{0.07})_2P$.

Acknowledgment

This work was done under a research project financed by erstwhile IUC-DAEF (now known as UGC-DAE Consortium for Scientific Research), Mumbai Centre, India. The same is gratefully acknowledged.

References

[1] Beckman O and Lundgren L 1991 *Handbook of Magnetic Materials* vol 6, ed K H J Buschow (Amsterdam: Elsevier)
[2] Fruchart R, Roger A and Senateur J P 1969 *J. Appl. Phys.* **40** 1250
[3] Fujii H, Hokabe T, Fujiwara H and Okamoto T 1978 *J. Phys. Soc. Japan* **44** 96
[4] Dolia S N, Krishnamurthy A, Ghose V and Srivastava B K 1993 *J. Phys.: Condens. Matter* **5** 451
[5] Maeda Y and Takashima Y 1973 *J. Inorg. Nucl. Chem.* **35** 1963
[6] Kumar S 2000 *PhD Thesis* University of Rajasthan, Jaipur
[7] Kumar S, Paranjpe S K, Srivastava B K and Krishnamurthy A 1999 *Phys. Status. Solidi* a **175** 693
[8] Zach R, Tobola J, Sredniawa B, Kaprzyk S, Casado C, Bacmann M and Fruchart D 2004 *J. Alloys Compounds* **383** 322
[9] Fruchart D, Allab F, Balli M, Gignoux D, Hill E K, Koumina A, Skryabina N, Tabola J, Wolfers P and Zach R 2005 *Physica* A **358** 123

[10] Tegus O, Bruck E, Buschow K H J and de Boer F R 2002 *Nature* **415** 150
[11] Jain S K, Kumar S, Krishna P S R, Shinde A B, Krishnamurthy A and Srivastava B K 2007 *J. Alloys Compounds* at press
[12] Sun N K, Li Y B, Li D, Zhang Q, Du J, Xiong D K, Zhang W S, Ma S, Liu J J and Zhang Z D 2007 *J. Alloys Compounds* **429** 29
[13] Paranjpe S K 1989 *Indian J. Pure Appl. Phys.* **27** 578
[14] Paranjpe S K and Dande Y D 1989 *Pramana J. Phys.* **32** 793
[15] Rodriguez-Carvajal J 2003 *FULLPROF version 3.0.0* Laboratorie Leon Brillouin, CEA-CNRS
[16] Watson R E and Freeman A J 1961 *Acta Crystallogr.* **14** 27
[17] Carlsson B, Ohrlin M and Rundqvist S 1973 *J. Solid State Chem.* **8** 5767
[18] Lundgren L, Tarmohamad G, Beckman O, Carlsson B and Rundqvist S 1978 *Phys. Scr.* **17** 39
[19] Fujii H, Hokabe T, Kamigaichi T and Okamoto T 1977 *J. Phys. Soc. Japan* **43** 41
[20] Wilkinson C, Wappling R and Ziebeck K R A 1989 *J. Magn. Magn. Mater.* **78** 269
[21] Fujii H, Komura S, Takeda T, Okamoto T, Ito Y and Akimitsu J 1979 *J. Phys. Soc. Japan* **46** 1616
[22] Scheerlinck D and Legrand E 1978 *Solid State Commun.* **25** 181
[23] Rhodes P and Wohlfarth E P 1963 *Proc. R. Soc.* A **273** 247
[24] Wohlfarth E P 1978 *J. Magn. Magn. Mater.* **7** 113